ACS OMEGA

http://pubs.acs.org/journal/acsodf

Article

Optical Immunosensor for the Detection of *Listeria monocytogenes* in Food Matrixes

Karthika Lakshmi Servarayan,[▽] Govindan Krishnamoorthy, Ellairaja Sundaram,[▽] Masiyappan Karuppusamy, Marudhamuthu Murugan, Shakkthivel Piraman, and Vairathevar Sivasamy Vasantha*

Cite This: *ACS Omega* 2023, 8, 15979−15989

Read Online

ACCESS | Metrics & More | Article Recommendations | Supporting Information

ABSTRACT: In this paper, simple imine-based organic fluorophore 4-amino-3-(anthracene-9 yl methyleneamino) phenyl (phenyl) methanone (APM) has been synthesized via a greener approach and the same was used to construct a fluorescent immunoassay for the detection of *Listeria monocytogenes* (LM). A monoclonal antibody of LM was tagged with APM via the conjugation of the amine group in APM and the acid group of anti-LM through EDC/NHS coupling. The designed immunoassay was optimized for the specific detection of LM in the presence of other interfering pathogens based on the aggregation-induced emission mechanism and the formation of aggregates and their morphology was confirmed with the help of scanning electron microscopy. Density functional theory studies were done to further support the sensing mechanism-based changes in the energy level distribution. All photophysical parameters were measured by using fluorescence spectroscopy techniques. Specific and competitive recognition of LM was done in the presence of other relevant pathogens. The immunoassay shows a linear appreciable range from 1.6×10^6−2.7024×10^8 cfu/mL using the standard plate count method. The LOD has been calculated from the linear equation and the value is found as 3.2 cfu/mL, and this is the lowest LOD value reported for the detection of LM so far. The practical applications of the immunoassay were demonstrated in various food samples, and their accuracy obtained was highly comparable with the standard existing ELISA method.

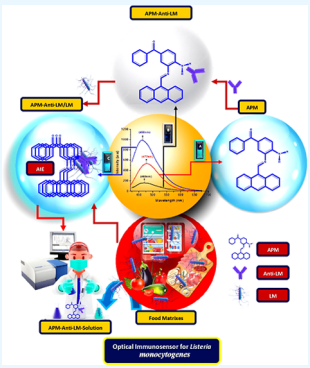

INTRODUCTION

Listeria monocytogenes (LM) is mostly witnessed as an important and third leading human pathogen which causes foodborne deaths in the USA.[1,2] In general, LM is a bacterial genus made up of Gram-positive round-end-shaped bacterium with short rods and they will occupy the cytoplasm of living cells.[3−5] LM species are widely present in the soil, water, feed, vegetation, farms, and industrial plants.[6−11] The main isolation source for LM is food materials such as milk products, seafood, vegetables, and raw and cooked meats[12−16] and hence the contamination has been initiated from these food origins.[17,18] LM is used to grow at temperatures ranging between −0.4 and 45 °C, at pH values of 5.0−9.6, and it has an ability to survive even at high salt concentrations and also low-water activity.[19−22] It mostly resists to certain preservative agents and thus makes its elimination from food very difficult.

In developed countries, LM readily occurs in ready-to-eat food as they have gained considerable popularity due to their better flavor, affordability, and accessibility.[23] Infections associated with LM could be categorized into non-invasive (febrile listerial gastroenteritis) and invasive (infection caused at sterile parts of the body such as the blood, liver, and cerebral fluid) listeriosis.[24,25] Non-invasive listeriosis shows severe symptoms like fever, diarrhea, headache, and muscle pain (myalgia) after a short incubation period when a healthy person intakes a high ingestion dose of the pathogenic *listeria*.[26−28] On the other hand, invasive listeriosis mainly affects the immune-suppressed young and elderly aged people like cancer patients, pregnant women, and acquired immunodeficiency syndrome patients.[29] Especially in pregnant women, it can cause premature labor, stillbirth, abortion, and neonatal infection, with high neonatal mortality.[30] As far as literature survey is concerned, the minimal infectious dose for LM is reported as 100 colony-forming units (cfu) per gram of food, and the general infection dose of LM for a healthy host will be in the range of 10^7−10^9 (cfu/g), and a range of 10^5 and 10^7 (cfu/g) has been witnessed as the risk of infection.[31] In developing countries like India, the foodborne diseases are contagious ones based on the seasons and plenty of milk, milk-derived products, meat, seafood, and vegetables have been reported to be contaminated as per the recent survey. Based on these serious health issues so far discussed above, we have chosen this bacteria for our studies and planned to design a

Received: December 9, 2022
Accepted: April 10, 2023
Published: April 24, 2023

Table 1. Comparison of the Performance of the Immunoassay with Existing Sensing Platforms for LM Bacteria

sensing material	detection technique	LOD (cfu/mL)	linear range (cfu/mL)	food matrixes	refs
monoclonal antibodies	fiber-optic	3×10^2		goat's cheese	63
Aptamer-A8	fiber-optic	1×10^3	10^3	sliced beef, chicken, and turkey	64
polyclonal antibodies	fiber optic	10^3		ready-to-eat beef, chicken, and turkey meats	65
Fe_3O_4 NPC	colorimetric	5.4×10^3	5.4×10^3–5.4×10^8	sterile milk samples	66
RAPTOR	fiber optic	5×10^5		frankfurter sample	67
UCNPs@GDN tannic acid, and hydrogen peroxide (HP)	fluorescent nanosystem	1.30×10^2	10^3 to 10^8	water, milk, and beef	68
polystyrene fiber	fiber-optic	4.3×10^3			69
CRISPR-Cas12a	fluorescence	10			70
Au@Pt nanozyme-mediated magnetic relaxation switching (MRS)	fluorescence	30	3×10^2–3×10^7	chicken sample	71
4-amino-3-(anthracen-9-ylmethyleneamino)phenyl(phenyl) methanone	fluorescence	3.2	1.6×10^6–2.7024×10^8	vegetables, milk and milk products, non-vegetarian foods, processed foods, and staple foods	current work

simple sensing assay to detect as well as quantify LM in food matrixes.

Generally, estimation of LM has been addressed as very difficult and in many cases, they are not declared precisely. On the point-of-need concern, already existing tests cannot be performed, and also, these tests require specialized laboratories and practices and leads to inefficient monitoring and control. Therefore, the rapid and sensitive LM bacterial detection is needed as a key element for efficient prevention of foodborne diseases[32] and also food industries require a new analytical tool or advanced detection methods to monitor LM bacterial contamination, which leads to food recalls and consequent economic losses, to meet the strict and specific regulatory guidelines on food security.[33]

Commonly, identification and quantification of bacteria mostly rely on conventional, culture-based methods, immunological-based assays, biochemical assays like agar plates, and microbroth dilution assays. However, these methods are inadequate to be performed in closed, confined spaces, as production plants. Mostly, culturing of pathogens requires an enrichment step in a broth followed by bacterial growth on agar plates, and also biochemical and physiological tests for strain identification. They are generally labor-intensive and most time-consuming. Sometimes more than 5 days may also be taken to provide initial results, and in some specific cases, it will take more than a week to confirm a specific pathogenic strain.

Currently existing developed traditional methods/techniques have been replaced with molecular approaches such as PCR amplification, DNA hybridization,[34] and ELISA-based techniques.[35] In general, PCR and DNA hybridization-based techniques are faster but need isolated genetic materials, specific instrumentation, trained personnel, and high cost, which is not suitable for clinical point-of-care usage. Nowadays, various and specific detection methods have been introduced for detecting LM in food samples, including loop-mediated isothermal amplification assays,[36] matrix-assisted laser desorption ionization time-of-flight (MALDI-TOF) mass spectroscopy,[37] and Fourier transform infrared (FT-IR) spectroscopy.[38−44] Though some remarkable advantages are reported, these methods lack various aspects such as calculating the number, biochemical characteristics, and colony identification, which are more time-consuming, and these immunological assays can suffer in specificity and hence false-positive results were noticed.[45] Moreover, these methods have been lacking in additional aspects like the amount of waste produced, long enrichment time, quantity and the use of expensive chemicals, and specialized equipment.[46]

Therefore, fast and sensitive immunoassays are extremely important and needed for the early prevention of food-based disease spreading associated with LM. Recently, electrochemical-based immunosensors have been reported which are the most promising techniques because of their high specificity, rapid analysis, and field deployable possibility.[47−50] Very recently, an electrochemical immunosensor was proposed by using an immobilized mouse monoclonal anti-*Listeria monocytogenes* antibody with graphene nanosheets chemically decorated with hybrid nanoparticles of a silver-ruthenium bipyridine complex core and a chitosan shell and has shown good response toward LM with a concentration range from 10^2 to 10^7 20 cells/mL and a detection limit of 2 cells/mL.[51] Though these electrochemical sensors have shown better sensitivity, they need multiple steps and require more than two materials to fabricate the electrodes of most of the electrochemical immunosensors used, lot of characterization techniques, and the need of some blocking agents to mask these electrodes. In recent years, fluorescence-based immunoassays have provided a good platform for designing good number of sensors with high potential, fast and high accuracy, direct detection, less time consumption, and minimum amount of reagents. Interestingly, fluorescence-based glutathione sensors have been reported in the system of the living being by using metal organic frameworks, such as $[Ru(bpy)_3]^{2+}$ encapsulated in UiO-66] coated with manganese dioxide nanosheets[52] [MnO_2 NS@$Ru(bpy)_3^{2+}$], using poly(thymine)-template fluorescent copper nanoparticles, a portable fluorescent sensor for the detection of organophosphorus pesticides with a detection limit of 3.33×10^{-5} ng/μL and a linear range of 1.00×10^{-4} −1.0 ng/μL,[53] and using MnO_2 nanosheets modified with 5-carboxyfluorescein for the determination of H_2O_2, glucose, and cholesterol.[54] Plenty of immunoassays have also been reported to date for various pathogenic bacteria and applied for human biofluids.[47] Likewise, some good number of immunoassays have been designed for LM (Table 1). A recently fluorescence sandwich-type immunoassay has been developed for LM using a chitosan-cellulose nanocrystal membrane with a detection limit of 10^2 cfu/mL.[55] Wang et al. have proposed a simple methodology by combining aptamer-coupled magnetic beads and IgG antibody-based dual recognition units for the

https://doi.org/10.1021/acsomega.2c07848
ACS Omega 2023, 8, 15979−15989

Scheme 1. Scheme Illustrating the Greener Synthesis of APM

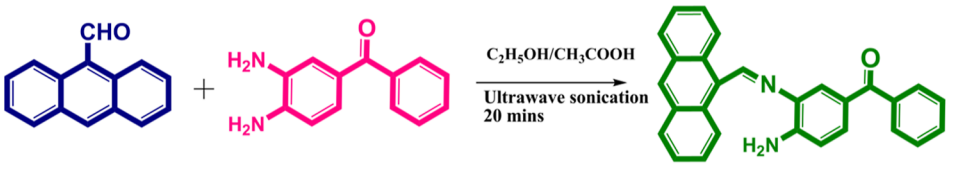

9-Anthracenecarboxaldehyde 3,4-Diaminobenzophenone 4-amino-3-(anthracene-9-ylmethyleneamino)phenyl)(phenyl)methanone

APM

detection of LM that gave a bright fluorescence signal due to the aggregation-induced emission with a limit of detection (LOD) and linear range of 10 and $10-10^6$ cfu/mL, respectively.[56] An aptamer-based sensor has been designed by Chen et al., which may be composed with two parts such as aptamer-functionalized up conversion magnetic nanoparticles with a linear range from 68 to 68×10^6 cfu/mL and a LOD of 8 cfu/mL.[57] Based on Pickering emulsion interfaces, LM was detected via molecularly imprinted polymer with CdTe quantum dots with a linear range from 10^3 to 10^5 cfu/mL and ended with a low detection limit of 10^3 cfu/mL.[58] Kaur et al., have detected LM by using peptide and gold nanoclusters. Herein, leucocin A peptide is used as a binding factor for LM bacteria, and the fluorescence signal was triggered on by gold nanoclusters with a LOD of 2×10^5 cfu mL^{-1}.[59]

Though plenty of nanoparticle-based sensing immunoassays have been reported, abovementioned immunoassays have mainly suffered due to reasons such as high-cost equipment, being more time-consuming, requiring complex operations, low sensitivity, or poor stability, which impede their further application. Therefore, there is an urgent need to establish a reliable and simple sensing method for the detection of LM bacteria with excellent sensitivity and selectivity.

Here, a simple and new fluorescence-based immunoassay for the selective detection of LM bacteria is proposed as the main objective of this research. In this regard, a simple fluorophore 4-amino-3-(anthracene-9 yl methyleneamino) phenyl (phenyl) methanone (APM) having an imine part which was synthesized via a one-pot greener approach using the ultrasonication method. The EDC/NHC tagging protocol was adapted to tag the APM probe with anti-LM. This Schiff base fluorophore-tagged anti-LM was utilized as a simple immunoassay platform for the detection of LM bacteria with the calculated linear range and LOD as from 1.6×10^6 to 2.7024×10^8 cfu/mL and 3.2 cfu/mL, respectively. The developed immunoassay has been applied for the quantification of LM bacteria in various food materials. This is the first organic fluorescent probe-based immunoassay for the detection of LM with lowest LOD as compared to that of other reported immunoassays.

METHODS AND TECHNIQUES

Methodology. Greener Synthesis of APM Using the Sonochemical Method

Currently, a simple imine was synthesized via the ultrawave sonication method. Briefly, 9-anthracenecarboxaldehyde (1 mmol) and 3,4-diamino benzophenone (1 mmol) were dissolved in 10 mL of absolute ethanol and stirred for 5 min and followed by the addition of 300 μL of glacial acetic acid with constant stirring. Then, the mixture was kept under a bath-type ultrawave sonicator (1.5 Hz) and sonicated for 20 min (Scheme 1). The completion of the reaction was confirmed by the appearance of a single spot corresponding to the product in TLC analysis. After that, the action mixture was poured into ice-cold water, and a light yellow precipitate was obtained. It was filtered, washed with diethyl ether, and finally dried over using anhydrous $CaCl_2$ under a vacuum chamber. It was recrystallized using absolute hot ethanol to obtain the pure product, and the yield was found to be 99.5% (1.98 g). As the reaction has utilized the simple sonication method, green solvents, good atom economy, and maximum product yield, our current approach is claimed as greener.

Structural Elucidation of APM. The structural characterization was done by using NMR, HR-MS, and FT-IR techniques, and the data are given below.

^{1}H and ^{13}C NMR spectra were recorded for APM and are shown in Figure S1a,b, respectively.

^{1}H NMR (500 MHz, [d_6] DMSO, 298 K): δ 7.79 (s, 1H), 7.14 (d, 2H), 6.77 (d, 4H), 6.63 (dd, 5H), 6.55−6.47 (m, 5H), 6.46 (s, 2H) in ppm.

^{13}C NMR: (500 MHz, [d_6] DMSO, 298 K): ^{13}C NMR (126 MHz, DMSO): δ 196.26 (s), 196.26 (s), 138.64 (s), 138.64 (s), 132.60 (s), 132.60 (s), 131.12 (s), 131.12 (s), 130.95 (s), 130.95 (s), 129.98 (s), 129.98 (s), 129.75 (s), 129.75 (s), 129.01 (d, J = 14.1 Hz), 127.59 (s), 126.20 (s), 125.87 (s), 125.49 (s).

The HR-MS study was carried out for APM and is shown in Figure S2.

$C_{23}H_{16}N_2$ (calculated mass—400.15): Observed mass −[M − H] = 400.15, yield: 98.5%.

The FT-IR analysis was done for APM and is shown in Figure S3.

FT-IR:IR spectra (in cm^{-1}): Imine (−CH═N−) and carbonyl (−C═O) 1652 cm^{-1}; primary amine ($-NH_2$) 3537 cm^{-1}; and C−N stretching 1296 cm^{-1}.

EDC/NHS Protocol for the Coupling of anti-LM with APM. The APM was tagged with anti-LM via the standard EDC/NHS coupling protocol. Briefly, 1 equiv of anti-LM (1 mL, 4.1 mg/1000 μL) in MES buffer and 4 equiv (4 mL, 0.001 M) of APM were mixed, and then, 100 μL of each EDC and NHS were added one by one to the above solution. It was gently stirred for 2 h and then kept for incubation at −4 °C for 1 h and stored at −4 °C in a deep freezer for 1 day for further use. Then, the resultant tagged anti-LM/APM (0.0082 mg/2000 μL) was allowed to stand at room temperature for 10 min, and then, it was centrifuged at 30,000 rpm for 20 min at −4 °C (Scheme 1). The resulting pellets were collected and washed thoroughly with PBS buffer five times. The unbounded APM was removed simply by washing with PBS buffer and confirmed by analyzing the supernatant solution using UV−vis spectra until the disappearance of the standard UV−vis peak of APM. The final APM/anti-LM in buffer solution was stored at −4 °C for further studies.[60]

https://doi.org/10.1021/acsomega.2c07848
ACS Omega 2023, 8, 15979−15989

Revival and Maintenance of Bacterial Cultures. The lyophilized cells of LM were grown initially in brain heart infusion broth (BHI broth) at 37 °C for 24 h and maintained LM in Luria Bertani broth (LB broth) at 37 °C. The lyophilized cells of *Salmonella. paratyphi*, *Klebsiella. pneumoniae*, *Staphylococcus. aureus*, *Escherichia coli*, and *Bacillus. cereus* were initially grown on nutrient agar (NA) at 37 °C and maintained in LB broth at 37 °C.

Viable Cell Number Analysis. The culture of LM was grown in LB broth at 37 °C for 16 h. After incubation, the bacterial culture was centrifuged at 10,000 rpm for 20 min. The cell pellet was washed thrice with PBS and Tween-20 buffers. The cells were resuspended and serially diluted in PBS solution, and the viable cell number was calculated using the most probable number method.

Designing of the Immunoassay (APM/anti-LM). The APM/anti-LM pellets were used for our immunoassay designing. These pellets were thoroughly dissolved in PBS buffer under constant stirring. 2 mL of the prepared APM/anti-LM (0.0082 mg) solution was mixed thoroughly with 10 μL of different diluted LM samples and kept under incubation for 25 min at 4 °C and 388 nm was fixed as the excitation wavelength for the throughout sensor studies, and the resulting fluorescence changes were recorded at 476 nm in PBS buffer solution.

Detection of LM in Real Food Samples. The main sources for LM are vegetables, milk and milk products, non-vegetarian foods, processed foods, and staple foods stored in the refrigerator. Different food samples (vegetable—carrot, ladies finger, potato, and tomato; milk; milk products—butter, cheese, curd, and paneer; non-vegetarian foods—chicken, egg, freshwater fish, seawater fish, prawn, and mutton; processed foods—bread, ice cream, and tomato sauce; and staple foods—chapati and boiled rice) were used to evaluate the applicability of the sensor in real samples. The food samples were collected from a local market named Vadapalanji, and the staple foods were procured from the university canteen, Madurai Kamaraj University. The solid food samples were weighed (5 g) and grounded using the mortar and pestle and resuspended in PBS with 0.05% to attain the final volume of 10 mL. Then, 10 mL of each real sample was transferred into different test tubes and inoculated with 1 mL of LM taken from 24 h old cultured LM and incubated at room temperature for 12 h.

Techniques. A Bruker 500 MHz spectrometer was used for basic ^{1}H and ^{13}C NMR studies using DMSO-[d_6] as solvent which contains a trace quantity of internal standard, tetramethylsilane, and the corresponding chemical shifts were reported in ppm at 25 °C. HR-MS spectra were measured using an Agilent HR-MS spectrometer. FT-IR spectra were measured using a Shimadzu FT-IR spectrometer. UV−visible spectra were recorded using the double beam UV−vis spectrophotometer (JASCO-V-730). Fluorescence measurements were carried out using a Cary Eclipse spectrophotometer having a 450 W xenon lamp and 5 and 2.5 nm were maintained as excitation and emission slit widths, respectively, throughout the experiments. The formation of the aggregates was confirmed by using a SEM instrument, TESCAN VEGA3 SBH.

Computational Methods. To gain insights into the geometry and electronic properties, density functional theory (DFT)-based calculations were carried out utilizing the Gaussian 16 (Revision A.03) suite of program. Initially, the relaxed potential energy scan was carried out to find the most stable (lowest energy) conformer. Subsequently, the most stable conformer was subjected to the optimization process. The APM geometry in the ground state was optimized without any symmetry constraints using hybrid Becke's three-parameter and Lee−Yang−Parr's gradient corrected correlation functional (B3LYP) in conjunction with Pople's split valence basis set with polarization functions [6-311G(d,p)]. The B3LYP functional is weighted at 20% exchange and 80% correlation. Moreover, the vibrational frequency analysis was carried out at the same level of theory to confirm the geometry as true minima on the potential energy surface. The molecular orbital contributions in the electronic transitions were simulated using the QM Forge package.

RESULTS AND DISCUSSION

Coupling of anti-LM with APM. We have utilized EDC/NHS coupling protocol for tagging anti-LM with the APM fluorophore via the formation of an amide bond. The coupling was confirmed based on the absorbance changes using UV−vis spectroscopy, and it assists us to confirm the formation of an amide bond. Absorption spectra for APM was recorded in a phosphate buffer medium and two major absorption peaks appeared at 266 and 388 nm, which may be due to $\pi-\pi^*$ and $n-\pi^*$ transitions, respectively (Figure S4). For coupling studies, MES and phosphate buffers were used, and the same coupling protocol adapted in our previous work was followed.[60] The peaks at 266 and 388 nm have been red-shifted to 300 and 401 nm, respectively, during the interaction with anti-LM. These spectral changes were observed because of the formation of an amide bond between the $-NH_2$ group of APM and the −COOH group of anti-LM[61] (Figure S5). The unbounded APM was removed by consecutive washing with PBS buffer and it was confirmed by UV−vis spectra (Figure S6). This anti-LM coupled APM has been used as a basic sensing platform of the developed immunoassay and these pellets were stored at −4 °C for further use.

Selective Studies of Fluorescent Immunoassay toward LM. Selectivity of the developed immunoassay was tested in presence of LM and other coexisting pathogenic bacteria like *E. Coli*, *S.paratyphi*, *B.cereus*, *S. aureus*, and *K. pneumoniae*. This kind of specific antibody-tagged fluorophores offers an excellent selectivity to recognize of LM.[60,61] First, the fluorescence nature of APM, APM/anti-LM, and APM/anti-LM/LM were recorded in PBS medium (Figure S7). APM has exhibited a maximum fluorescence intensity at 477 nm which is mainly due to the transfer of charge (CT) from the donor amine groups of benzophenone to the acceptor anthracene part, which was supported by the DFT study. After addition of antibody LM to the PBS solution containing APM, the fluorescence intensity of the above peak decreased with the slight blue shift from 477 to 469 nm. When anti-LM is introduced, this CT is inhibited due to the formation of the amide bond and this may increase the energy levels between molecules and hence a slight blue shift is noted. To the same mixture, when LM was added, the fluorescence intensity increased drastically and doubled compared to the emission intensity of pure APM with a blue shift from 477 to 460 nm. This was due to the formation of an immunocomplex and further increases the energy levels. Hence, the blue shift seems to be caused by an energy-transfer process that is related to the complex formation between APM/anti-LM and LM.[62] At the same time, when the other interfering pathogenic bacteria were

https://doi.org/10.1021/acsomega.2c07848
ACS Omega 2023, 8, 15979−15989

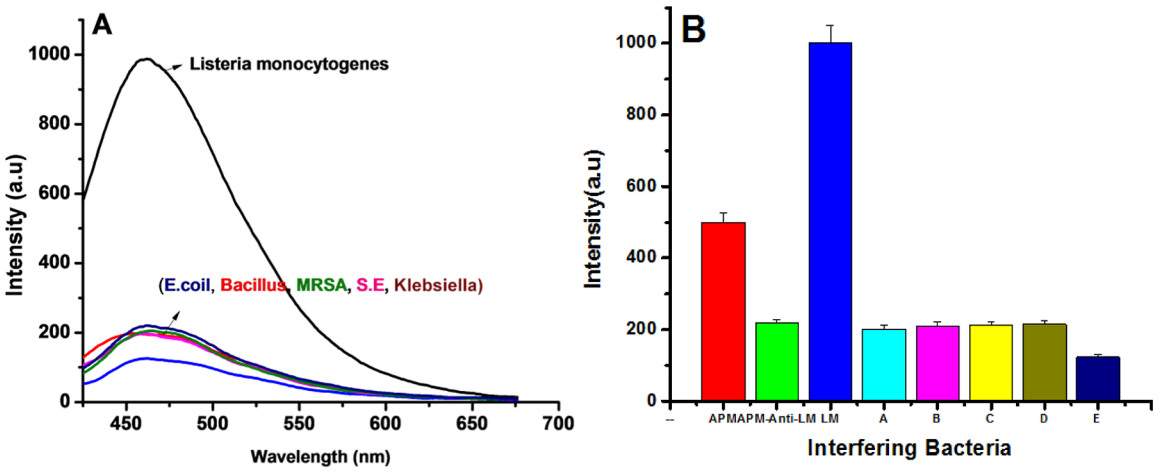

Figure 1. Specific fluorescence response of APM/anti-LM toward LM in the presence of other pathogens (A) and the corresponding bar diagram (B) (Concentration of APM is 0.001 M; bulk concentration of anti-LM is 4.1 mg/1000 μL and APM/anti-LM is 0.0082 mg/2000 μL; LM and other pathogens are 10^{-1} cfu/g in PBS buffer pH = 7.4; incubation time is 5 min). [(A) *E. coli*, (B) *B. cereus*, (C) *S. paratyphi*, (D) *S. aureus*, and (E) *K. pneumoniae*].

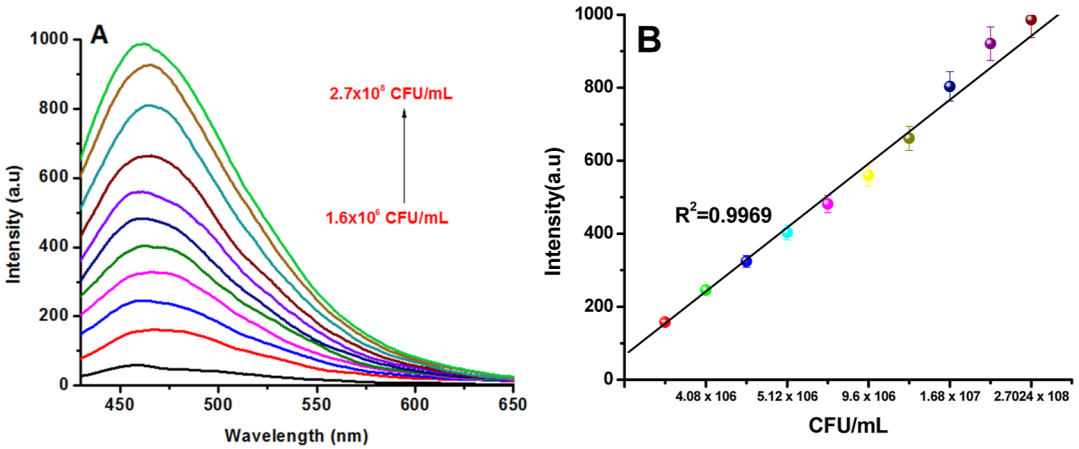

Figure 2. Emission response of APM/anti-LM while varying the concentrations of LM bacteria (A), and corresponding linear regression plot (B) (concentration of APM is 0.001 M; bulk concentration of anti-LM is 4.1 mg/1000 μL and APM/anti-LM is 0.0082 mg/2000 μL; LM is 1.6×10^8 to 2.710^6 in PBS buffer pH = 7.4).

added to the solution containing APM/anti-LM, no increment in the emission intensity was observed as for LM addition instead there was a slight decrement in the emission intensity. It shows that the APM/anti-LM platform has strong selective interactions with LM (Figure 1). This kind of a fluorescence immunosensing platform does not need any blocking agents as in the case of the electrochemical immunoassay.[60] This phenomenon shows the applicability of the developed immunoassay for the detection of LM in various food matrixes selectively in the presence of other interfering bacteria.

Quantification of LM using APM/anti-LM. The developed immunoassay has shown an excellent emission response as well as visible color change for LM under a UV lamp (Figure S8). In order to quantify or find out the sensitivity of the developed immunoassay, the parent culture was diluted in a serial manner from 10^{-1} to 10^{-10} times and the same bacterial solution was used to quantify LM by using the immunoassay platform. There was a gradual increment in the fluorescence intensity observed with the addition of the above bacterial solutions and the corresponding emission data are given in Figure 2. From the fluorescence intensity data, the cfu was calculated using the standard plate counting method[61] for the respective dilution factors (10^{-1} to 10^{-10}). The developed immunoassay has covered a wide range of detection from 1.6×10^6 to 2.7024×10^8 cfu/mL and the LOD has been calculated as 3.2 cfu/mL. When the linear range of the developed immunoassay is compared with that of previous nanoparticle-based fluorescence platforms, our report is comparable and sometimes better than that of earlier reports. However, the LOD of our sensing platform is lowest than the earlier reports (Table 1). This is the first organic fluorescent probe-based immunoassay for the detection of LM.

In general, using the ELISA plate count method, one could count the cfu up to two digits for any bacterial detection. In this study, the developed immunoassay detected the LM up to 3.2 cfu/mL. This is one of the most remarkable advantages of this immunoassay.

Competitive Response Study of the Developed Fluorescence Immunoassay. As the food matrixes are contaminated with more than one microorganism, thus we have cross-checked the selectivity through a competitive response study of the immunoassay in the presence of all other interfering pathogenic microorganisms in the same solution. In detail, 1 equiv of all interfering pathogens was

https://doi.org/10.1021/acsomega.2c07848
ACS Omega 2023, 8, 15979−15989

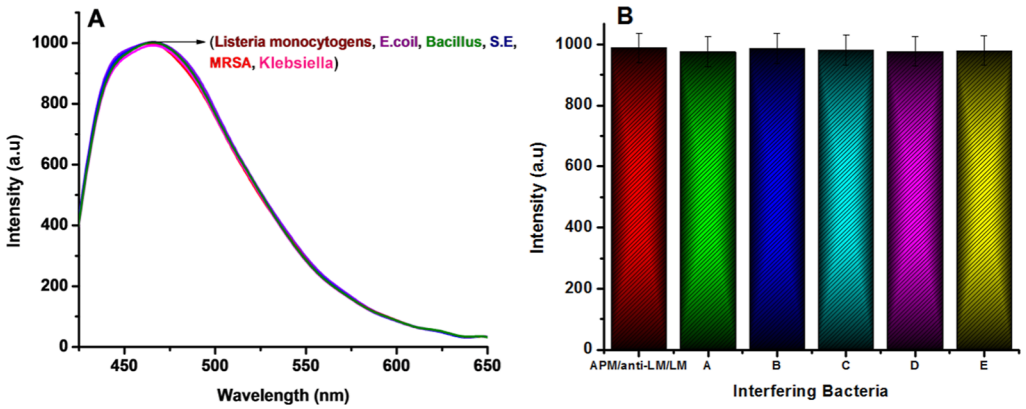

Figure 3. Competitive study of the developed immunoassay, APM/anti-LM toward LM in the presence of relevant pathogenic bacteria (A), and corresponding bar diagram (B) [(A) *E. coli*, (B) *E. coli* + *B. cereus*, (C) *E. coli* + *B. cereus* + *S. paratyphi*, (D) *E. coli* + *B. cereus* + *S. paratyphi* + *S.aureus*, and (E) *E. coli* + *B.cereus* + *S. paratyphi* + *S. aureus* + *K. pneumoniae*] (Concentration of APM is 0.001 M; bulk concentration of anti-LM is 4.1 mg/1000 μL and APM/anti-LM is 0.0082 mg/2000 μL; LM and other pathogens are 10^{-1} cfu/g in PBS buffer pH = 7.4; incubation time is 5 min.)

Scheme 2. Scheme Illustrating the Tentative Mechanism of Detection of LM Using APM/Anti-LM

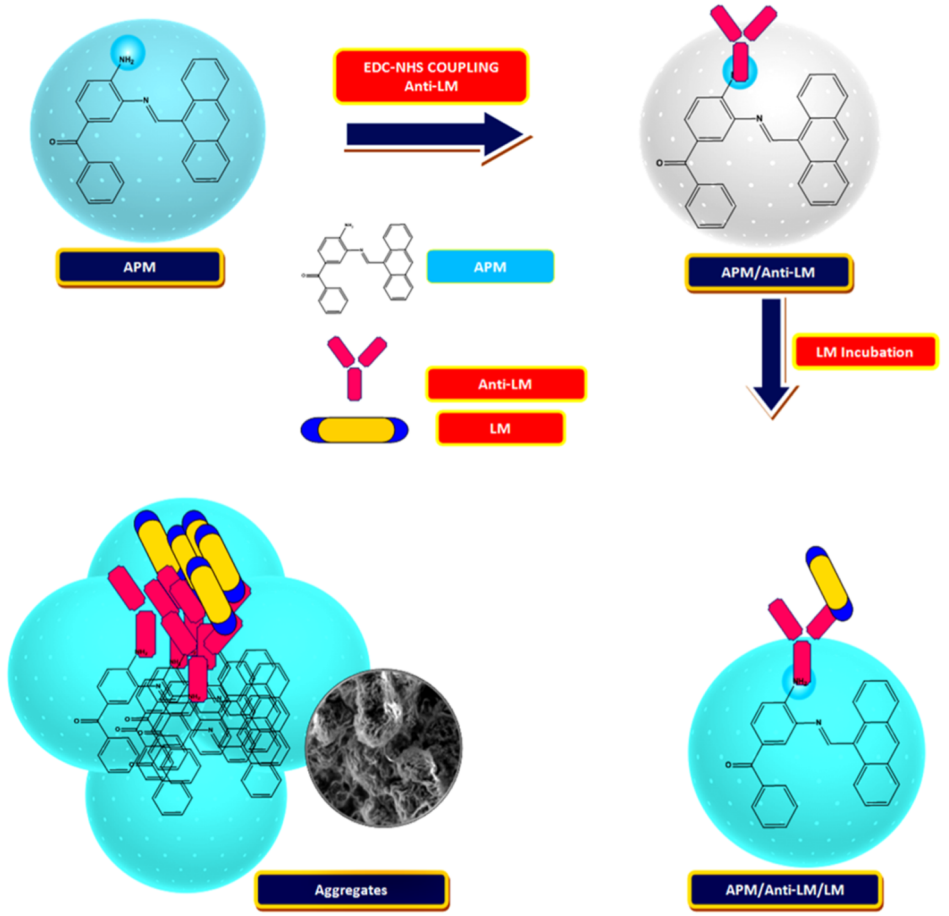

added one by one to the solution containing 1 equiv of APM/anti-LM/LM and incubated for 5 min at −4 °C for each addition. The corresponding fluorescence responses were recorded. No change in fluorescence intensity was observed and all the graphs overlapped with each other (Figure 3). Hence, the developed immunoassay could be a promising immunoassay platform for the detection of LM in any contaminated real samples.

Proposed Sensing Mechanism of the Developed Immunoassay. In general, an intra/intermolecular charge-transfer-based mechanism has been widely existing in most of the reported organic-based fluorescence-sensing assays.[72−74] In the current study, the probe has exhibited a maximum fluorescent intensity at 477 nm which is mainly due to the CT from the donor amine groups of benzophenone to the acceptor anthracene part, which was supported by the DFT study.[75] After tagging APM with anti-LM, an amide bond was

https://doi.org/10.1021/acsomega.2c07848
ACS Omega 2023, 8, 15979−15989

formed between the donor amine group and carboxyl group of antibody and hence the charge transfer between donor and acceptor groups was inhibited and hence there was quenching of the emission intensity. When LM was introduced into the sensing solution, LM may be forming immunocomplexes with APM/anti-LM part. Due this complex formation, the distance between the anthracene part of the complex is decreased which induces dimerization followed by aggregation of the complexes (Scheme 2). The formation of the aggregation is responsible for the above drastic increase in the emission intensity. This kind of phenomenon was absorbed by many research groups.[76−80] This aggregation-induced emission mechanism was further supported by SEM and the corresponding image is given in Figure S9.

Computational Analysis. The ground-state geometry of APM is optimized in the gas phase and the same is depicted in Figure 4. The Cartesian coordinates of the geometry and

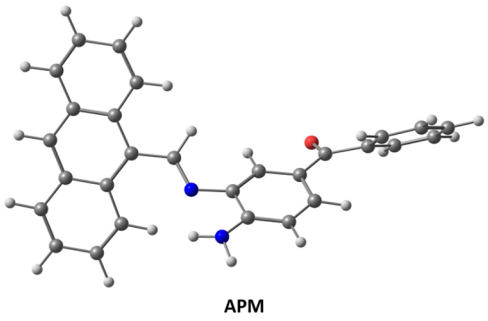

Figure 4. round-state optimized geometry of the APM molecule.

calculated frontier molecular orbitals and energy gap (E_g) of APM are shown in Figure 5. The highest occupied molecular

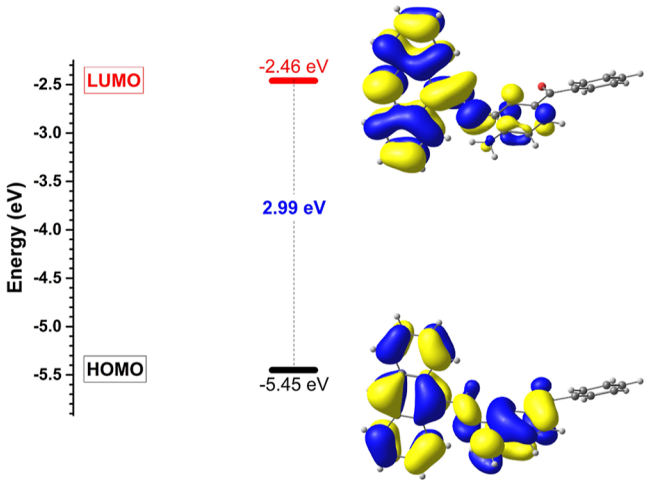

Figure 5. alculated frontier molecular orbital with energy levels at the B3LYP/6-311G(d,p) level of theory. The isodensity surface contour value is set to be 0.02 au.

orbital (HOMO) and lowest unoccupied molecular orbital (LUMO) should be localized over donor and acceptor groups to form an efficient charge-separated state, respectively.[81−84] It is clear from Figure 5 that the electron densities of HOMO are predominantly localized over anthracene and amino benzophenone groups. In contrast, in the case of LUMO, the electron densities are centered more on the anthracene group. It indicates that the APM molecule exhibits moderate charge separation. The HOMO, LUMO, and energy gap values for the APM molecule are −5.45, −2.46 and 2.99 eV, respectively.

The molecular orbital contribution of electron density for each atom was calculated at the same level of theory based on the C-squared population analysis to analyze the trend of electron transfer between the donor and acceptor groups.[84] We considered the amino benzophenone group as a donor and the anthracene group as an acceptor. The molecular orbital contribution from the HOMO of donor and acceptor groups is 50.72 and 49.28%, respectively. On the other hand, the contribution from the LUMO of the donor and acceptor moieties is 24.91 and 75.09%, respectively. The HOMO values of the donor are higher than that of the HOMO values of the acceptor. It indicates the possibility of electron transfer from donor to acceptor groups.

Detection of LM in Food Matrixes. As LM mostly grows in refrigerated food samples, hence we have collected more number of food samples including vegetables, rice, chapati, meat, egg, fish, and dairy products like milk, cheese, paneer, butter, and ice cream, and tomato sauce. The samples were prepared as mentioned in the materials and methods section. Under optimized conditions, the fluorimetric titrations were performed by the addition of LM with known dilution factors to the food samples and the corresponding fluorescence intensity changes were recorded. In all the cases, increments in the fluorescence intensity were observed and the corresponding graphs are shown in Figure S10. From the standard linear plot (Figure 2B), the corresponding cfu/mL values of LM in the respective food samples were calculated. The same experiments were repeated using the ELISA method and the efficiency of the developed immunoassay was compared and the data are given in Table 2. The immunoassay has shown a good data agreement with the ELISA method. This developed

Table 2. Detection of LM Inoculated Food Samples by Using Our Developed Immunoassay and the Standard Plate Count Method

sl. no.	food sample	detection of LM in real samples using APM/anti-LM (cfu/mL)	detection of LM in real samples using ELISA/plate count method (cfu/mL)
1	carrot	1.52×10^6	1.6×10^6
2	ladies finger	4.2×10^6	5.12×10^6
3	potato	1×10^6	LTC
4	tomato	3.5×10^6	4.08×10^6
5	tomato sauce	4.12×10^6	4.5×10^6
6	rice	0.9×10^6	LTC
7	milk	4.52×10^6	5×10^6
8	curd	7.975×10^7	8.73×10^9
9	cheese	1×10^6	LTC
10	paneer	4.73×10^6	4.37×10^6
11	butter	4.21×10^6	4.96×10^6
12	bread	5×10^6	5.12×10^6
13	ice cream	1.2×10^6	1.75×10^6
14	chapati	3.52×10^6	4.08×10^6
15	chicken	5.17×10^6	5.32×10^6
16	egg	1.2×10^6	LTC
17	mutton	4.9×10^6	5.12×10^6
18	seawater fish	7.6×10^6	8.16×10^6
19	freshwater fish	1.2×10^6	1.65×10^6
20	prawn	4.8×10^6	5.15×10^6

https://doi.org/10.1021/acsomega.2c07848
ACS Omega 2023, 8, 15979−15989

immuno protocol involves cheaper sensing materials and has quick response unlike the ELISA method, which involves costly enzymes and is time-consuming to quantify LM.

In this work, a simple and greener methodology was followed for the synthesis of imine-based fluorophores for designing an immunoassay to detect LM in food matrixes. This imine has exhibited a good fluorescence property and it also possesses good binding site for the coupling with anti-LM. As a result, the designed immunoassay platform has shown an excellent specificity for LM among the presence of interfering bacteria and also has shown a wide linear range of detection from 1.6×10^6 to 2.7024×10^8 cfu/mL and LOD has been found as 3.2 cfu/mL. The LOD obtained in our study is the best report compared to earlier reports. However, the linear range of our study is comparable with some earlier reports and this may be limited to some other pathogens in the *Listeria* family. The immunoassay has provided a novel protocol for the determination of LM in various food matrixes and also exhibited good compatibility with the existing biological methods of detection.

■ ASSOCIATED CONTENT

Supporting Information

The Supporting Information is available free of charge at https://pubs.acs.org/doi/10.1021/acsomega.2c07848.

Materials; NMR spectra; HR-MS spectrum; FT-IR spectrum; UV−vis and emission spectral data; SEM analysis; and real sample analysis (PDF)

■ AUTHOR INFORMATION

Corresponding Author

Vairathevar Sivasamy Vasantha − *Department of Natural Products Chemistry, School of Chemistry, Madurai Kamaraj University, Madurai 625021 Tamil Nadu, India;* orcid.org/0000-0001-8391-8682; Email: vasantham999@yahoo.co.in

Authors

Karthika Lakshmi Servarayan − *Department of Natural Products Chemistry, School of Chemistry, Madurai Kamaraj University, Madurai 625021 Tamil Nadu, India*

Govindan Krishnamoorthy − *Translational Research Platform for Veterinary Biologicals, Central University Laboratory, TANUVAS, Chennai 600051 Tamil Nadu, India*

Ellairaja Sundaram − *Department of Chemistry, Vivekananda College, Madurai 625234, India*

Masiyappan Karuppusamy − *Centre for High Computing, CSIR-Central Leather Research Institute, Adyar, Chennai 600020, India; Academy of Scientific and Innovative Research (AcSIR), Ghaziabad 201002, India;* orcid.org/0000-0001-9811-2585

Marudhamuthu Murugan − *Department of Microbial Technology, Madurai Kamaraj University, Madurai 625021, India;* orcid.org/0000-0002-1624-5374

Shakkthivel Piraman − *Department of Nanoscience and Technology, Alagappa University, Karaikudi 630003, India;* orcid.org/0000-0003-4081-2823

Complete contact information is available at: https://pubs.acs.org/10.1021/acsomega.2c07848

Author Contributions

[▽]K.L.S. and E.S. equally contributed.

Notes

The authors declare no competing financial interest.

■ ACKNOWLEDGMENTS

This work was financially supported by RUSA Phase II Scheme, New Delhi, India (grant no.: 007-R2/RUSA/MKU/2020−2021). Hence, the author K.L.S. has registered her thanks to RUSA for offering the fellowship for pursuing her Ph.D. program. The author also thanks DST PURSE, FTST, IRHPA School of Chemistry, and Central Instrumentation Facility, Madurai Kamaraj University for offering NMR spectrofluorimeter and SEM facilities. M.K. gratefully acknowledges the Council of Scientific and Industrial Research (CSIR) for the CSIR-SRF fellowship (grant no.: 31/006(0470)/2020-EMR-I, dated 12/10/2020) and the use of the supercomputing resources at CSIR-4PI. The authors thank Dr. V. Subramanian, Visiting Professor, IIT Madras for his suggestions on DFT calculations. CSIR-CLRI Communication no.: 1821.

■ REFERENCES

(1) Chiriacò, M.; Parlangeli, I.; Sirsi, F.; Poltronieri, P.; Primiceri, E. Impedance Sensing Platform for Detection of the Food Pathogen Listeria Monocytogenes. *Electron* **2018**, *7*, 347.

(2) Soni, D. K.; Ahmad, R.; Dubey, S. K. Biosensor for the detection of Listeria Monocytogenes: emerging trends. *Crit. Rev. Microbiol.* **2018**, *44*, 590−608.

(3) Wang, W.; Liu, L.; Song, S.; Xu, L.; Zhu, J.; Kuang, H. Gold nanoparticle-based paper sensor for multiple detection of 12 Listeria spp. by P60-mediated monoclonal antibody. *Food Agric. Immunol.* **2017**, *28*, 274−287.

(4) Orsi, R. H.; Wiedmann, M. Characteristics and distribution of Listeria spp., including Listeria species newly described since 2009. *Appl. Microbiol. Biotechnol.* **2016**, *100*, 5273−5287.

(5) Kayode, A. J.; Igbinosa, E. O.; Okoh, A. I. Overview of listeriosis in the Southern African Hemisphere-Review. *J. Food Saf.* **2020**, *40*, No. e12732.

(6) Lyautey, E.; Lapen, D. R.; Wilkes, G.; McCleary, K.; Pagotto, F.; Tyler, K.; Hartmann, A.; Piveteau, P.; Rieu, A.; Robertson, W. J.; Medeiros, D. T.; Edge, T. A.; Gannon, V.; Topp, E. Distribution and Characteristics of *Listeria Monocytogenes* Isolates from Surface Waters of the South Nation River Watershed, Ontario, Canada. *Appl. Environ. Microbiol.* **2007**, *73*, 5401−5410.

(7) Lakicevic, B.; Nastasijevic, I.; Raseta, M. Sources of *Listeria Monocytogenes* contamination in retail establishments. *Procedia Food Sci.* **2015**, *5*, 160−163.

(8) Watkins, J.; Sleath, K. P. Isolation and enumeration of *Listeria Monocytogenes* from sewage, sewage sludge and river water. *J. Appl. Bacteriol.* **1981**, *50*, 1−9.

(9) Caro, M. R.; Zamora, E.; Leon, L.; Cuello, F.; Salinas, J.; Megias, D.; Cubero, M.; Contreras, A. Isolation and identification of *Listeria Monocytogenes* in vegetable byproduct silages containg preservative additives and destined for animal feeding. *Anim. Feed Sci. Technol.* **1990**, *31*, 285−291.

(10) Destro, M. T.; Leitao, M. F.; Farber, J. M. Use of molecular typing methods to trace the dissemination of *Listeria Monocytogenes* in a shrimp processing plant. *Appl. Environ. Microbiol.* **1996**, *62*, 1852−1853.

(11) Kimura, B. Recent Advances in the Study of the Genotypic Diversity and Ecology of Listeria monocytogenes. *Microbes Environ.* **2006**, *21*, 69−77.

(12) Jami, M.; Ghanbari, M.; Zunabovic, M.; Domig, K. J.; Kneifel, W. *Listeria Monocytogenes* in aquatic food products-a review. *Compr. Rev. Food Sci. Food Saf.* **2014**, *13*, 798−813.

(13) Moosavy, M.-H.; Esmaeili, S.; Mostafavi, E.; Bagheri Amiri, F. Isolation of *Listeria Monocytogenes* from milks used for Iranian traditional cheese in Lighvan cheese factories. *Ann. Agric. Environ. Med.* **2014**, *21*, 728−729.
(14) Brown, L. G.; Hoover, E. R.; Ripley, D.; Matis, B.; Nicholas, D.; Hedeen, N.; Faw, B. Retail deli slicer cleaning frequency−six selected sites, United States, 2012. *Morb. Mortal. Wkly. Rep.* **2016**, *65*, 306−310.
(15) Luo, L.; Zhang, Z.; Wang, H.; Wang, P.; Lan, R.; Deng, J.; Miao, Y.; Wang, Y.; Wang, Y.; Xu, J.; et al. A 12-month longitudinal study of *Listeria Monocytogenes* contamination and persistence in pork retail markets in China. *Food Control* **2017**, *76*, 66−73.
(16) Ballesteros, L.; Moreno, Y.; Cuesta, G.; Rodrigo, A.; Tomás, D.; Hernández, M.; Ferrús, M. A.; Henández, J. G. Persistence of *Listeria Monocytogenes* strains in a frozen vegetables processing plant determined by serotyping and REP-PCR. *Int. J. Food Sci. Technol.* **2011**, *46*, 1109−1112.
(17) Gebretsadik, S.; Kassa, T.; Alemayehu, H.; Huruy, K.; Kebede, N. Isolation and characterization of *Listeria Monocytogenes* and other *Listeria* species in foods of animal origin in AddisAbaba, Ethiopia. *J. Infect. Public Health* **2011**, *4*, 22−29.
(18) Dowe, M. J.; Jackson, E. D.; Mori, J. G.; Bell, C. R. *Listeria Monocytogenes* survival in soil and incidence in agricultural soils. *J. Food Prot.* **1997**, *60*, 1201−1207.
(19) (a) Gandhi, M.; Chikindas, M. L. Review: Listeria: A foodborne pathogen that knows how to survive. *Int. J. Food Microbiol.* **2007**, *113*, 1−15. (b) Hossein-Nejad-Ariani, H.; Kim, T.; Kaur, K. Peptide-based biosensor utilizing fluorescent gold nanoclusters for detection of Listeria Monocytogenes. *ACS Appl. Nano Mater.* **2018**, *1*, 3389−3397.
(20) Duffy, G.; Sheridan, J. J. The effect of temperature, pH and medium in a surface adhesion immunofluorescent technique for detection of *Listeria Monocytogenes*. *J. Appl. Microbiol.* **1997**, *83*, 95−101.
(21) Miettinen, M. K.; Björkroth, K. J.; Korkeala, H. Characterization of *Listeria Monocytogenes* from an ice cream plant by serotyping and pulsed-field gel electrophoresis. *Int. J. Food Microbiol.* **1999**, *46*, 187−192.
(22) Freitag, N. E.; Port, G. C.; Miner, M. D. *Listeria Monocytogenes*-from saprophyte to intracellular pathogen. *Nat. Rev. Microbiol.* **2009**, *7*, 623−628.
(23) Asiegbu, C. V.; Lebelo, S. L.; Tabit, F. T. The food safety knowledge and microbial hazards awareness of consumers of ready-to-eat street-vended food. *Food Control* **2016**, *60*, 422−429.
(24) Bhat, S. A.; Willayat, M. M.; Roy, S. S.; Bhat, M. A.; Shah, S. N.; Ahmed, A.; Maqbool, S.; Ganayi, B. A. Isolation, molecular detection and antibiogram of *Listeria Monocytogenes* from human clinical cases and fish of Kashmir, India. *Comp. Clin. Pathol.* **2013**, *22*, 661−665.
(25) Zhu, Q.; Gooneratne, R.; Hussain, M. *Listeria Monocytogenes* in fresh produce: Outbreaks, prevalence and contamination levels. *Foods* **2017**, *6*, 21−32.
(26) Donovan, S. Listeriosis: a rare but deadly disease. *Clin. Microbiol. Newsl.* **2015**, *37*, 135−140.
(27) Lamont, R. F.; Sobel, J.; Mazaki-Tovi, S.; Kusanovic, J. P.; Vaisbuch, E.; Kim, S. K.; Uldbjerg, N.; Romero, R. Listeriosis in human pregnancy: a systematic review. *J. Perinat. Med.* **2011**, *39*, 227−236.
(28) Halbedel, S.; Prager, R.; Banerji, S.; Kleta, S.; Trost, E.; Nishanth, G.; Alles, G.; Hölzel, C.; Schlesiger, F.; Pietzka, A.; et al. A *Listeria Monocytogenes* ST2 clone lacking chitinase ChiB from an outbreak of non-invasive gastroenteritis. *Emerg. Microb. Infect.* **2019**, *8*, 17−28.
(29) Desai, A. N.; Anyoha, A.; Madoff, L. C.; Lassmann, B. Changing epidemiology of *Listeria Monocytogenes* outbreaks, sporadic cases, and recalls globally: A review of ProMED reports from 1996 to 2018. *Int. J. Infect. Dis.* **2019**, *84*, 48−53.
(30) Mylonakis, E.; Paliou, M.; Hohmann, E. L.; Calderwood, S. B.; Wing, E. J. Listeriosis during pregnancy: A case series and review of 222 cases. *Medicine* **2002**, *81*, 260−269.
(31) Buchanan, R. L.; Gorris, L. G. M.; Hayman, M. M.; Jackson, T. C.; Whiting, R. C. A review of Listeria Monocytogenes:an update on outbreaks, virulence, dose-response, ecology, and risk assessments. *Food Control* **2017**, *75*, 1−13.
(32) Vidic, J.; Manzano, M.; Chang, C.-M.; Jaffrezic-Renault, N. Advanced biosensors for detection of pathogens related to livestock and poultry. *Vet. Res.* **2017**, *48*, 11−33.
(33) Vizzini, P.; Braidot, M.; Vidic, J.; Manzano, M. Electrochemical and Optical Biosensors for the Detection of *Campylobacter* and *Listeria*: An Update Look. *Micromachines* **2019**, *10*, 500−514.
(34) Yan, L.; Zhao, W.; Wen, Z.; Li, X.; Niu, X.; Huang, Y.; Sun, W. Electrochemical DNA Sensor for hly Gene of *Listeria Monocytogenes* by Three-Dimensional Graphene and Gold anocomposite Modified Electrode. *Int. J. Electrochem. Sci.* **2017**, *12*, 4086−4095.
(35) Cavaiuolo, M.; Paramithiotis, S.; Drosinos, E. H.; Ferrante, A. Development and optimization of an ELISA based method to detect *Listeria Monocytogenes* and Escherichia coli O157 in fresh vegetables. *Anal. Methods* **2013**, *5*, 4622−4627.
(36) Kil, E. J.; Kim, S.; Lee, Y. J.; Kang, E. H.; Lee, M.; Cho, S.; Kim, M. K.; Lee, K. Y.; Heo, N. .Y.; Choi, H. S.; Kwon, S. T.; Lee, S. Advanced loop-mediated isothermal amplification method for sensitive and specific detection of Tomato chlorosis virus using a uracil DNA glycosylase to control carry-over contamination. *J. Virol. Methods* **2015**, *213*, 68−74.
(37) Barbuddhe, S. B.; Maier, T.; Schwarz, G.; Kostrzewa, M.; Hof, H.; Domann, E.; Chakraborty, T.; Hain, T. Rapid Identification and Typing of *Listeria* Species by Matrix-Assisted Laser Desorption Ionization−Time of Flight Mass Spectrometry. *Appl. Environ. Microbiol.* **2008**, *74*, 5402−5407.
(38) Wenning, M.; Scherer, S. Identification of microorganisms by FTIR spectroscopy: perspectives and limitations of the method. *Appl. Microbiol. Biotechnol.* **2013**, *97*, 7111−7120.
(39) Rebuffo, C. A.; Schmitt, J.; Wenning, M.; von Stetten, F.; Scherer, S.; Schmitt, J.; Wenning, M.; Stetten, F. V.; Scherer, S. Reliable and Rapid Identification of *Listeria Monocytogenes* and *Listeria* Species by Artificial Neural Network-Based Fourier Transform Infrared Spectroscopy. *Appl. Environ. Microbiol.* **2006**, *72*, 994−1000.
(40) Rebuffo-Scheer, C. A.; Schmitt, J.; Scherer, S. Differentiation of *Listeria Monocytogenes* using Artificial Neural Network Analysisof Fourier Transformed Infrared Spectra. *Appl. Environ. Microbiol.* **2007**, *73*, 1036−1040.
(41) Al-Mariri, A.; Ramadan, L.; Abou Younes, A.; Al-Laham, A. Identification of Listeria Species by Fourier-transform Infrared Spectroscopy. *Bulg. J. Vet. Med.* **2019**, *22*, 285−296.
(42) Janbu, A. O.; Moretro, T.; Bertrand, D.; Kohler, A. FT-IR microspectroscopy: a promising method for the rapid identification of Listeria species. *FEMS Microbiol. Lett.* **2008**, *278*, 164−170.
(43) Xu, J. L.; Herrero-Langreo, A.; Lamba, S.; Ferone, M.; Scannell, A. G.; Caponigro, V.; Gowen, A. A. Characterisation and Classification of Foodborne Bacteria Using Reflectance FTIR Microscopic Imaging. *Molecules* **2021**, *26*, 6318.
(44) Davis, R.; Mauer, L. J. Fourier-transform Infrared (FT-IR) Spectroscopy: A Rapid Tool for Detection and Analysis of Foodborne Pathogenic Bacteria. *Current research, technology and education topics in applied microbiology and microbial biotechnology*; Formatex Research Cente, 2010; Vol. 2, pp 1582−1594.
(45) Embarek, P. K. B. Presence, detection and growth of Listeria monocytogenes in seafoods: a review. *Int. J. Food Microbiol.* **1994**, *23*, 17−34.
(46) Soni, D. K.; Ahmad, R.; Dubey, S. K. Biosensor for the detection of Listeria monocytogenes: Emerging Trends. *Crit. Rev. Microbiol.* **2018**, *44*, 590−608.
(47) Tully, E.; Higson, S. P.; O'Kennedy, R. The development of a 'labeless' immunosensor for the detection of Listeria monocytogenes cell surface protein, Internalin B. *Biosens. Bioelectron.* **2008**, *23*, 906−912.
(48) Wang, R.; Ruan, C.; Kanayeva, D.; Lassiter, K.; Li, Y. TiO2 nanowire bundle microelectrode based impedance immunosensor for

https://doi.org/10.1021/acsomega.2c07848
ACS Omega 2023, 8, 15979−15989

rapid and sensitive detection of Listeria monocytogenes. *Nano Lett.* **2008**, *8*, 2625−2631.
(49) Radhakrishnan, R.; Jahne, M.; Rogers, S.; Suni, I. I. Detection of Listeria monocytogenes by electrochemical impedance spectroscopy. *Electroanalysis* **2013**, *25*, 2231−2237.
(50) Bhardwaj, J.; Devarakonda, S.; Kumar, S.; Jang, J. Development of a paper-based electrochemical immunosensor using an antibody-single walled carbon nanotubes bio-conjugate modified electrode for label-free detection of foodborne pathogens. *Sens. Actuators, B* **2017**, *253*, 115−123.
(51) Veerapandian, M.; Neethirajan, S. Graphene oxide chemically decorated with Ag−Ru/chitosan nanoparticles: fabrication, electrode processing and immunosensing properties. *RSC Adv.* **2015**, *5*, 75015−75024.
(52) Zhu, S.; Wang, S.; Xia, M.; Wang, B.; Huang, Y.; Zhang, D.; Zhang, X.; Wang, G. intracellular Imaging of Glutathione with MnO2 Nanosheet@Ru(bpy)$_3^{2+}$-UiO-66 Nanocomposites. *ACS Appl. Mater. Interfaces* **2019**, *11*, 31693−31699.
(53) Chen, J.; Han, T.; Feng, X.; Wang, B.; Wang, G. A poly (thymine)-templated fluorescent copper nanoparticle hydrogel-based visual and portable strategy for an organophosphorus pesticide assay. *Analyst* **2019**, *144*, 2423−2429.
(54) Han, T.; Zhu, S.; Wang, S.; Wang, B.; Zhang, X.; Wang, G. Fluorometric methods for determination of H_2O_2, glucose and cholesterol by using MnO2 nanosheets modified with 5-carboxy-fluorescein. *Microchim. Acta* **2019**, *186*, 269.
(55) Capo, A.; D'Auria, S.; Lacroix, M. A fluorescence immunoassay for a rapid detection of Listeria Monocytogenes on working surfaces. *Sci. Rep.* **2020**, *10*, 21729.
(56) Guo, Y.; Zhao, C.; Liu, Y.; Nie, H.; Guo, X.; Song, X.; Xu, K.; Li, J.; Wang, J. A novel fluorescence method for the rapid and effective detection of *Listeria Monocytogenes* using aptamer-conjugated magnetic nanoparticles and aggregation-induced emission dots. *Analyst* **2020**, *145*, 3857−3863.
(57) Liu, R.; Zhang, Y.; Ali, S.; Haruna, S. A.; He, P.; Li, H.; Ouyang, Q.; Chen, Q. Development of a fluorescence aptasensor for rapid and sensitive detection of *Listeria Monocytogenes* in food. *Food Control* **2021**, *122*, 107808.
(58) Zhao, X.; Cui, Y.; Wang, J.; Wang, J. Preparation of Fluorescent Molecularly Imprinted Polymers via Pickering Emulsion Interfaces and the Application for Visual Sensing Analysis of Listeria Monocytogenes. *Polymers* **2019**, *11*, 984.
(59) Hossein-Nejad-Ariani, H.; Kim, T.; Kaur, K. Peptide-Based Biosensor Utilizing Fluorescent Gold Nanoclusters for Detection of *Listeria monocytogenes*. *ACS Appl. Nano Mater.* **2018**, *1*, 3389−3397.
(60) Sundaram, E.; Kathiravan, S.; Manna, A.; Chinnaiah, A.; Vasantha, V. S. Designing of New Optical Immunosensors Based on 2-Amino-4-(anthracen-9-yl)-7-hydroxy-4 H-chromene-3-carbonitrile for the Detection of Aeromonas hydrophila in the Organs of Oreochromis mossambicus Fingerlings. *ACS Omega* **2019**, *4*, 4814−4824.
(61) Ellairaja, S.; Krithiga, N.; Ponmariappan, S.; Vasantha, V. S. Novel pyrimidine tagged silver nanoparticle based fluorescent immunoassay for the detection of Pseudomonas aeruginosa. *J. Agric. Food Chem.* **2017**, *65*, 1802−1812.
(62) Riegler, J.; Ditengou, F.; Palme, K.; Nann, T. Blue shift of CdSe/ZnS nanocrystal-labels upon DNA-hybridization. *J. Nanobiotechnol.* **2008**, *6*, 7.
(63) Mendonca, M.; Conrad, N. L.; Conceicao, F. R.; Moreira, A. N.; da Silva, W. P.; Aleixo, J. A.; Bhunia, A. K. Highly specific fiber optic immunosensor coupled with immunomagnetic separation for detection of low levels of Listeria Monocytogenes and L. ivanovii. *BMC microbial* **2012**, *12*, 275.
(64) Ohk, S. H.; Koo, O. K.; Sen, T.; Yamamoto, C. M.; Bhunia, K. A. Antibody−aptamer functionalized fibre-optic biosensor for specific detection of *Listeria monocytogenes* from food. *Food Microbiol.* **2010**, *109*, 808−817.
(65) Ohk, S.-H.; Bhunia, A. K. Multiplex fiber optic biosensor for detection of Listeria monocytogenes, Escherichia coli O157: H7 and Salmonella enterica from ready-to-eat meat samples. *J. Appl. Microbiol.* **2013**, *33*, 166−171.
(66) Zhang, L.; Huang, R.; Liu, W.; Liu, H.; Zhou, X.; Xing, D. Rapid and visual detection of *Listeria monocytogenes* based on nanoparticle cluster catalyzed signal amplification. *Biosens. Bioelectron.* **2016**, *86*, 1−7.
(67) Nanduri, V.; Kim, G.; Morgan, M. T.; Ess, D.; Hahm, B. K.; Kothapalli, A.; Valadez, A.; Geng, T.; Bhunia, A. Antibody immobilization on waveguides using a flow−through system shows improved *Listeria monocytogenes* detection in an automated fiber optic biosensor: RAPTOR. *Sensors* **2006**, *6*, 808−822.
(68) Yin, M.; Wu, C.; Li, H.; Jia, Z.; Deng, Q.; Wang, S.; Zhang, Y. Simultaneous sensing of seven pathogenic bacteria by guanidine-functionalized upconversion fluorescent nanoparticles. *ACS Omega* **2019**, *4*, 8953−8959.
(69) Geng, T.; Morgan, M. T.; Bhunia, A. K. Detection of low levels of *Listeria monocytogenes* cells by using a fiber-optic immunosensor. *Appl. Environ. Microbiol.* **2004**, *70*, 6138−6146.
(70) Tian, Y.; Liu, T.; Liu, C.; Xu, Q.; Fang, S.; Wu, Y.; Wu, M.; Liu, Q. An ultrasensitive and contamination-free on-site nucleic acid detection platform for *Listeria Monocytogenes* based on the CRISPR-Cas12a system combined with recombinase polymerase amplification. *LWT* **2021**, *152*, 112166.
(71) Wu, Z.; Huang, C.; Dong, Y.; Zhao, B.; Chen, Y. Gold core@ platinum shell nanozyme-mediated magnetic relaxation switching DNA sensor for the detection of *Listeria Monocytogenes* in chicken samples. *Food Control* **2022**, *137*, 108916.
(72) Valeur, B.; Leray, I. Design principles of fluorescent molecular sensors for cation recognition. *Coord. Chem. Rev.* **2000**, *205*, 3−40.
(73) De Silva, A. P.; Gunaratne, H. Q. N.; Gunnlaugsson, T.; Huxley, A. J.; McCoy, C. P.; Rademacher, J. T.; Rice, T. E. Signaling recognition events with fluorescent sensors andswitches. *Chem. Rev.* **1997**, *97*, 1515−1566.
(74) Lu, C.; Xu, Z.; Cui, J.; Zhang, R.; Qian, X. Ratiometric and highly selective fluorescent sensor for cadmium under physiological pH range: a new strategy to discriminate cadmium from zinc. *J. Org. Chem.* **2007**, *72*, 3554−3557.
(75) Chudomel, J. M.; Yang, B.; Barnes, M. D.; Achermann, M.; Mague, J. T.; Lahti, P. M. Highly twisted triarylamines for photoinduced intramolecular charge transfer. *J. Phys. Chem. A* **2011**, *115*, 8361−8368.
(76) Rajamalli, P.; Senthilkumar, N.; Gandeepan, P.; Huang, P. Y.; Huang, M. J.; Ren-Wu, C. Z.; Yang, C. Y.; Chiu, M. J.; Chu, L. K.; Lin, H. W.; et al. A new molecular design based on thermally activated delayed fluorescence for highly efficient organic light emitting diodes. *J. Am. Chem. Soc.* **2016**, *138*, 628−634.
(77) Gao, M.; Tang, B. Z. Fluorescent sensors based on aggregation-induced emission: recent advances and perspectives. *ACS Sens.* **2017**, *2*, 1382−1399.
(78) Zhang, Y.; Xu, H.; Ma, X.; Shi, Z.; Yin, J.; Jiang, X. Self-Assembly of Amphiphilic Anthracene-Functionalized β-Cyclodextrin (CD-AN) through Multi-Micelle Aggregation. *Macromol. Rapid Commun.* **2016**, *37*, 998−1004.
(79) Tong, H.; Hong, Y.; Dong, Y.; Häussler, M.; Li, Z.; Lam, J. W.; Dong, Y.; Sung, H. H. Y.; Williams, I. D.; Tang, B. Z. Protein detection and quantitation by tetraphenylethene-based fluorescent probes with aggregation-induced emission characteristics. *J. Phys. Chem. B* **2007**, *111*, 11817−11823.
(80) Huang, L.; Dai, L. Aggregation-Induced Emission for Highly Selective and Sensitive Fluorescent Biosensing and Cell Imaging. *J. Polym. Sci., Part A: Polym. Chem.* **2017**, *55*, 653−659.
(81) Frisch, M. J.; Trucks, G. W.; Schlegel, H. B.; Scuseria, G. E.; Robb, M. A.; Cheeseman, J. R.; Scalmani, G.; Barone, V.; Petersson, G. A.; Nakatsuji, H.; Li, X.; Caricato, M.; Marenich, A. V.; Bloino, J.; Janesko, B. G.; Gomperts, R.; Mennucci, B.; Hratchian, H. P.; Ortiz, J. V.; Izmaylov, A. F.; Sonnenberg, J. L.; Williams; Ding, F.; Lipparini, F.; Egidi, F.; Goings, J.; Peng, B.; Petrone, A.; Henderson, T.; Ranasinghe, D.; Zakrzewski, V. G.; Gao, J.; Rega, N.; Zheng, G.; Liang, W.; Hada, M.; Ehara, M.; Toyota, K.; Fukuda, R.; Hasegawa, J.;

https://doi.org/10.1021/acsomega.2c07848
ACS Omega 2023, 8, 15979−15989

Ishida, M.; Nakajima, T.; Honda, Y.; Kitao, O.; Nakai, H.; Vreven, T.; Throssell, K.; Montgomery, J. A., Jr.; Peralta, J. E.; Ogliaro, F.; Bearpark, M. J.; Heyd, J. J.; Brothers, E. N.; Kudin, K. N.; Staroverov, V. N.; Keith, T. A.; Kobayashi, R.; Normand, J.; Raghavachari, K.; Rendell, A. P.; Burant, J. C.; Iyengar, S. S.; Tomasi, J.; Cossi, M.; Millam, J. M.; Klene, M.; Adamo, C.; Cammi, R.; Ochterski, J. W.; Martin, R. L.; Morokuma, K.; Farkas, O.; Foresman, J. B.; Fox, D. J. *Gaussian 16*, 2016; Vol. *16*, p 03.

(82) (a) Becke, A. D. Density-functional thermochemistry. III. The role of exact exchange. *J. Chem. Phys.* **1993**, *98*, 5648−5652. (b) Lee, C.; Yang, W.; Parr, R. G. Development of the Colle-Salvetti correlation-energy formula into a functional of the electron density. *Phys. Rev. B* **1988**, *37*, 785−789. (c) Ditchfield, R.; Hehre, W. J.; Pople, J. A. Self-Consistent Molecular-Orbital Methods. IX. An Extended Gaussian-Type Basis for Molecular-Orbital Studies of Organic Molecules. *J. Chem. Phys.* **1971**, *54*, 724−728.

(83) Tenderholt, A. L. *QMForge: A Program to Analyze Quantum Chemistry Calculations*, Version 2.3, 2007; Vol. 2.

(84) Karuppusamy, M.; Choutipalli, V. S. K.; Vijay, D.; Subramanian, V. Rational Design of Novel N-doped Polyaromatic Hydrocarbons as Donors for the Perylene based Dye-Sensitized Solar Cells. *J. Chem. Sci.* **2020**, *132*, 20.

https://doi.org/10.1021/acsomega.2c07848
ACS Omega 2023, 8, 15979−15989